Journal of Power Sources 201 (2012) 219–225

Contents lists available at SciVerse ScienceDirect

Journal of Power Sources

journal homepage: www.elsevier.com/locate/jpowsour

Heterogeneous through-plane distributions of polytetrafluoroethylene in polymer electrolyte membrane fuel cell gas diffusion layers

A. Rofaiel, J.S. Ellis, P.R. Challa, A. Bazylak*

Microscale Energy Systems Transport Phenomena Laboratory, Department of Mechanical and Industrial Engineering, Faculty of Applied Science & Engineering, University of Toronto, 5 Kings College Road, Toronto, Ontario, Canada, M5S 3G8

ARTICLE INFO

Article history:
Received 29 September 2011
Received in revised form 31 October 2011
Accepted 1 November 2011
Available online 7 November 2011

Keywords:
Polymer electrolyte membrane fuel cell
Gas diffusion layer
Polytetrafluoroethylene (PTFE)
Wettability distribution
Heterogeneous

ABSTRACT

Polytetrafluoroethylene (PTFE) has been widely employed as a hydrophobic coating for the polymer electrolyte membrane fuel cell (PEMFC) gas diffusion layer (GDL). Despite a number of application techniques available, a method of quantifying the distribution of PTFE in the through-plane direction of the GDL has not been well established. In this work, we present a novel method for measuring heterogeneous through-plane PTFE distributions within the bulk of the GDL using scanning electron microscopy (SEM) energy dispersive X-ray spectrometry (EDS) imaging. To the authors' best knowledge, this work represents the first direct experimental investigation of the through-plane distributions of PTFE for various commercially available GDLs. SEM EDS imaging of typical PTFE distributions for paper, felt, and cloth GDLs are presented and discussed. SEM backscatter electron images (SEI) are also provided to enable the comparison of PTFE distributions with the morphological features of the GDL. This work has the potential to be employed to tune PTFE distributions for optimal water management in the GDL for improving the overall design and performance of PEMFCs.

1. Introduction

Polymer electrolyte membrane fuel cells (PEMFCs) are highly efficient, scalable devices for the conversion of chemical to electrical energy [1]. One of the major challenges in improving PEMFC performance is water management [2–4]. One component that plays an important role in such water management is the gas diffusion layer (GDL), a hydrophobic porous carbon fiber layer that aids in (i) reactant delivery to the catalyst layer, (ii) removal of liquid water, and (iii) improving the electronic conductivity and structural stability of the MEA. Accumulation of liquid water in the GDL can limit fuel cell performance by blocking reactant access to the catalyst layer, and must be removed to prevent clogging of the GDL pores [2,4,5]. The issue of water management can be addressed by understanding the transport properties of the GDL. Porosity and hydrophobicity are two such properties that require further study.

Commercially available GDLs can be classified into three categories based on their microstructure: paper, felt and cloth. Polyacrylonitrile-based carbon fibers are either bonded together in a matrix (paper), hydro-entangled (felt), or woven (cloth). For paper, individual carbon fibers are cut to lengths of 3–12 mm, bound into a web-like structure using a binder (typically polyvinyl alcohol), impregnated with resin, and finally heat-treated to temperatures over 2000 °C [5]. For felt, the fibers are bound together by a hydro-entanglement step that orients some of the fibers in the through-plane direction, in the absence of a binder. Both felt and paper morphologies are highly porous (typical pore size is between 10 and 30 μm [5]). The fiber placement in felt is more random due to the hydro-entanglement process. For cloth GDLs, the carbon fibers are formed into yarn strands that are woven into a cloth structure. For cloth, the weave pattern tends to produce both macro- and micro-pores, compared to the micro-porous structure of paper and felt [2,6]. As Escribano et al. [7] observed, these microstructural variations influence the properties of GDLs.

GDLs are rendered hydrophobic by applying a polytetrafluoroethylene (PTFE) coating. PTFE is a fluoropolymer consisting of a repeating carbon backbone with fluorine side units, having composition $(C_2F_4)_n$. It is well-suited for application to the GDL due to its hydrophobicity and stability [5,8]. Typically, carbon black is added to improve the electrical conductivity of the coating. Borup et al. [9] observed that the GDL loses its hydrophobicity with time, and Schulze et al. correlated the GDL performance loss with changes in its surface properties [10]. The objective of the present study is to compare through-plane distributions of PTFE in paper, felt, and cloth GDLs to help improve our understanding of the GDL surface properties. To this end, we describe a microscopy technique to probe the elemental composition of GDL cross-sections impregnated with PTFE.

* Corresponding author. Tel.: +1 416 946 5031; fax: +1 416 978 7753.
E-mail address: abazylak@mie.utoronto.ca (A. Bazylak).

0378-7753/$ – see front matter © 2011 Elsevier B.V. All rights reserved.
doi:10.1016/j.jpowsour.2011.11.005

Lim and Wang found that when varying the PTFE content of paper GDL Toray TGP-H-090, a 10 wt.% addition of PTFE provided desirable fuel cell performance [11]. (For the remainder of this paper, we refer to Toray TGP-H-90 as T090). It is important to note that Lim and Wang only investigated paper GDL. As well, they applied the PTFE treatment in-house, and did not examine pre-treated GDLs. Although PTFE increases the hydrophobicity of the GDL, its application should be limited due to its high electrical resistivity (greater than $10^{18}\ \Omega\,cm^{-1}$) [12]. Another tradeoff to PTFE application is the impact on GDL porosity distributions [2,13], which in turn can influence the mass transport behavior within the fuel cell.

While 10 wt.% PTFE was found to be sufficient by Lim and Wang [11] when they studied T090, 20 wt.% is the highest generally employed PTFE loading [5]. Through an analysis of GDL microstructure parameters such as porosity, absolute permeability, and contact angle, Park and Popov [2] determined that the optimal PTFE content was approximately 20 wt.%. They found that optimal performance is based on a balance between the hydrophobicity of the GDL surface and its absolute permeability. However, a recent review by Wang et al. [14] has stated that further studies are required to fully characterize the hydrophilic/hydrophobic distribution within the GDL, and that this information is required for realistic model development and numerical analysis.

There are several methods of applying a hydrophobic treatment to the GDL. Since PTFE resin does not respond well to solvent or melting processes [15], it is usually applied as an aqueous dispersion. The dispersion contains PTFE particle sizes ranging from 50 to 500 nm [16]. Since typical GDLs pore sizes are between 10–30 μm [5], the PTFE particles should easily penetrate into the GDL bulk. Typical PTFE application techniques include spray, brush, flow, and immersion of the GDL in a PTFE solution [2,5]. Spray and brush techniques are better suited for surface or one-sided applications, while the immersion and flow methods are more effective when bulk treatment is required. PTFE bulk penetration is important so that liquid water does not remain trapped within the porous core region of the GDL. Since most commercial and experimental purposes require bulk PTFE distribution, the immersion technique is the most common. Immersion also allows for a greater control on the applied PTFE content (PTFE loading), as the dispersion concentrations can be adjusted. Additionally, PTFE can be repeatedly applied until the desired weight loading is achieved. A key drawback to this method is the lack of control of PTFE distribution, particularly in the through-plane orientation. For a description of PTFE application processes, the reader is referred to the available literature [2,5,16,17].

Although several researchers have investigated the impact of PTFE loading on overall PEMFC performance [2,8,11,18], the quantification of its effect has been mostly limited to overall loading. The PTFE application process has the potential to affect the through-plane porosity distribution. Mathias et al. [5] reported that changing the drying time during PTFE application can affect its distribution, with slower drying times leading to higher concentrations in the interior of the GDL, and faster drying times showing higher concentrations near the surfaces. Lobato et al. [8] showed that increasing PTFE loading also increases the electrical resistivity, in both the in-plane and through-plane directions.

Literature regarding the graded application of PTFE in through-plane and in-plane orientations is sparse. As mentioned above, Mathias et al. [5] provided measurements of through-plane distributions in relation to PTFE dispersion drying times. However, the particular effects of the distributions were not discussed, nor were standard methodologies for reproducing such distributions developed. The difficulty in performing such measurements is due to the heterogeneity of the GDL morphology and PTFE distribution. The GDL is highly porous, and the distribution of PTFE at one location may vary significantly from those in other locations. Large pores can also act to conceal areas of PTFE coverage, yielding inaccurate coverage data. In a recent study, Mendoza et al. [19] used Raman spectroscopy to measure in-plane PTFE distributions in carbon paper GDLs. The authors analyzed the carbon and fluorine signatures at both high and low concentrations of PTFE. The presence of PTFE was detected at loadings down to 1.8 wt.% PTFE, and large features were observed for loadings above 20 wt.%. However, they did not consider through-plane distributions of PTFE, which is important as this is the direction of water transport between the catalyst layer and the current-collecting bipolar plate, nor did they explore the PTFE content for other GDL microstructures.

To characterize through-plane distributions of PTFE for a range of GDL materials, we present an imaging method that employs scanning electron microscopy (SEM) energy dispersive X-ray spectrometry elemental mapping (EDS). SEM EDS is a surface imaging technique for determining the presence of particular elements. A high-energy electron beam is focused on a surface, exciting electrons of near-surface atoms, which emit photons. Emitted X-rays from the element of interest, which have a selective characteristic energy, are detected and mapped based on their relative intensities, to produce a visual representation of the element's presence on the surface. The resulting image is a two-dimensional map showing the locations of the element of interest. Due to PTFE's high concentration of fluorine and its absence in the regular structure of the GDL, fluorine is a suitable element for determining the presence of PTFE. The characteristic energy of fluorine is 0.677 keV. From the two-dimensional elemental mappings obtained from the EDS measurements, we generate one-dimensional through-plane PTFE distributions, illustrating their dependence on the heterogeneous GDL microstructures.

Recently, Radhakrishnan and Haridoss [20] used a similar technique to characterize the presence of PTFE in the residue obtained from compressing a GDL over multiple cycles. They found that this cyclic compression led to degradation of PTFE within the GDL due to the applied pressure. Although that technique is similar to the work discussed in the present paper, to the best of our knowledge, this is the first direct experimental investigation to qualitatively compare the through-plane PTFE distributions in three commercially available GDL microstructures: paper, felt, and cloth.

2. Methodology

2.1. Sample preparation

Untreated GDLs were obtained from the following manufacturers: Freudenberg H2315 (felt), Toray TGP-H-090 (paper), and AvCarb 1071 HCB (cloth). For PTFE treatment, samples were sent to Fuel Cell Earth (Stoneham, MA) to ensure a uniform PTFE application process for all samples. However, the process of PTFE application is proprietary. The benefit of purchasing commercially available materials is that materials that would be used in fuel cell applications can be analyzed.

For each material, untreated and 10 wt.% PTFE treated samples were tested (Table 1). The samples were initially cut to approximately 1 cm × 1 cm and mounted in extension springs to stand upright and parallel, as shown in Fig. 1a. The springs and samples

Table 1
Identification and properties of the GDL samples tested.

Material	Manufacturer	PTFE loading [wt.%]	Thickness [μm]
Felt	Freudenberg H2315	10	150–200
Paper	Toray TGP-H 090	10	200–250
Cloth	AVCarb 1071 HCB	10	250–300

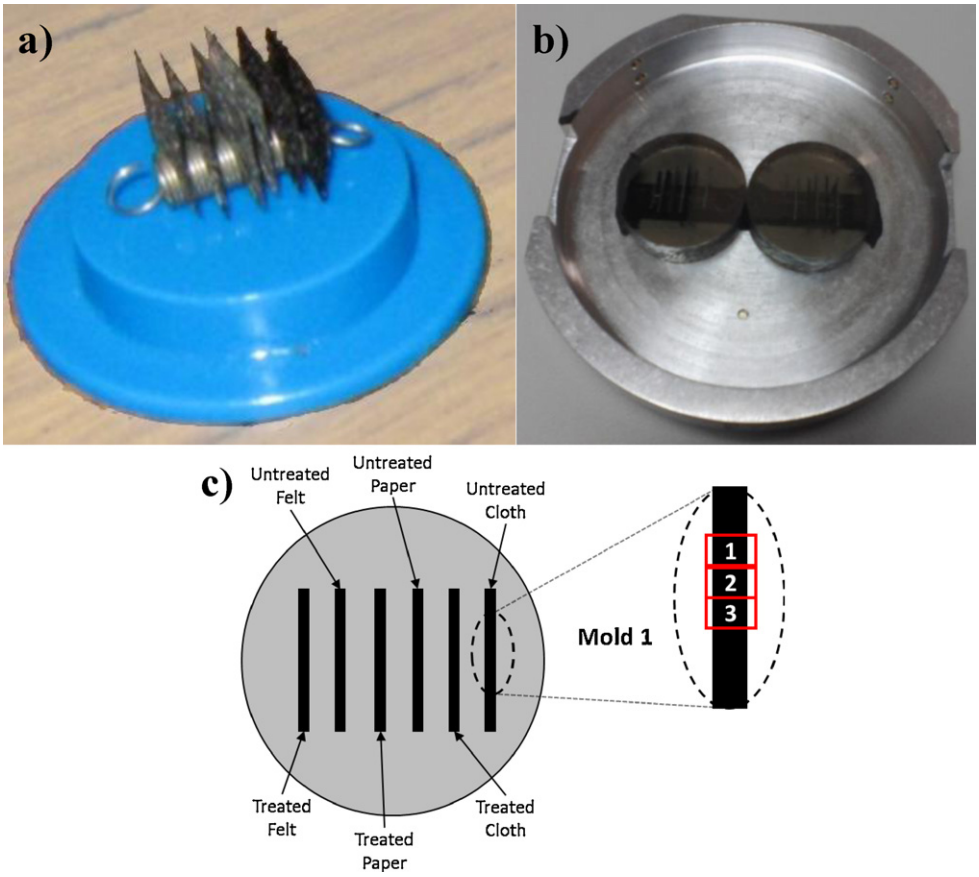

Fig. 1. GDL sample holders: (a) GDL samples mounted in an extension spring to hold the samples in place for mold 1. (b) The two molds in their final state (following ultrasonic cleaning and carbon coating) held in the SEM loading plate by conductive carbon tape. (c) Sample placement and imaging locations for mold 1.

were placed in a mold plate, and Epo-Thin low-viscosity epoxy hardener and resin (Buehler, Whitby, Canada; 5 parts resin to 2 parts hardener) was added to the mold-plate until the GDL samples were submerged; the epoxy was then allowed to cure. The epoxy molds were used purely to immobilize the GDL samples for SEM imaging, and it is unlikely that the epoxy would have any effect on the structure or the PTFE distributions. For each microstructure and treatment combination, two samples of each material were prepared and placed in separate molds, so each sample-treatment measurement was repeated. Because the resin contains substantial quantities of chlorine, this signature element can be used to distinguish the resin from the PTFE (primarily fluorine) and GDL (primarily carbon).

After allowing the resin to cure for over 24 h, the mold was ground and polished using three levels of fine, oil-based mono-crystalline diamond suspensions (15 μm, 9 μm, and 1 μm, sequentially) until the surfaces of the GDL were exposed. The polishing process took several hours by way of a manual rubbing motion, using slow and gentle motions. This technique of slow and even polishing was employed to ensure that there was no damage to the GDL samples.

After polishing, the samples were sonicated in hexane for approximately 5 min to remove any contaminants. Due to the porosity of the GDL, sonication was necessary to remove remnant impurities and particles from the polishing process. The samples were then sputter-coated with carbon (carbon evaporation coating at 80 Å), for enhanced electronic conductivity for examination under the SEM. Fig. 1b shows the mold in its final form, with the through-plane surface of each sample exposed and carbon coated.

2.2. EDS measurements

EDS elemental mapping was employed for determining the presence of fluorine within the GDL. Due to the high concentration of fluorine in PTFE and its absence in the GDL, fluorine is a suitable element for determining the presence of PTFE throughout the GDL. Through X-ray radiation, excited electrons emit photons at a characteristic wavelength (1.832 nm for fluorine). These photons are detected and mapped based on relative intensities to produce a visual representation of the presence of fluorine. All SEM imaging was performed on a JEOL JSM-6610LV SEM with an Oxford Instruments X-max Silicon Drift Detector with 20 mm^2 active area for EDS measurements. PTFE-treated samples were examined with EDS maps for quantifying fluorine content and SEI for illustrating the structural morphology of the GDL. An untreated felt sample was imaged at the characteristic wavelength of fluorine, and no signal was detected. This demonstrated that the technique was indeed measuring fluorine in the PTFE.

To mitigate shadowing due to GDL porosity and maximize penetration of the beam into the pores, the samples were oriented parallel to the vertical (azimuth) angle of the EDS beam. When capturing the EDS maps, both fluorine and carbon maps were examined.

The imaging regions were taken adjacent to each other, so that a continuous region was captured. This is shown schematically in Fig. 1c. Multiple images were collected for each sample, and the distributions were averaged and normalized. The reported results were representative of observed trends. It is important to note that some variation is expected between samples due to the randomness of the GDL structure [13].

The SEM magnification varied between 250× and 350×, depending on the sample thickness (between approximately 150 and 300 μm). The size of the EDS image was 512 × 384 pixels acquired with a pixel dwell time of 600 μs for a total capture time of 117.96 s per frame. Each image was obtained through software-based frame integration of 5 frames.

The fluorine map images were condensed into one-dimensional distributions using MATLAB's Image Processing Toolbox. The greyscale value of each pixel along the in-plane direction of the image (horizontal axis in the EDS mappings) was summed to obtain a relative PTFE value along the thickness of the GDL. The relative PTFE values were normalized across the through-plane direction.

3. Results

As discussed above in Section 2, two molds were constructed for immobilizing the GDLs for SEM imaging. However, the imaging results were found to be qualitatively similar, so we focus only on Mold 1 for the remainder of the paper. For Mold 1, the imaged regions were adjacent to each other, so that a continuous image was formed across the entire scan length (Fig. 1c).

Fig. 2 shows the SEI SEM images of the felt (a), paper (b), and cloth (c), for the GDL materials and treatments described in Table 1. It is important to note that the SEI results clarify the local morphological structure of the material, consisting of carbon fibers, PTFE and resin (and binder, in the case of paper GDL). EDS maps of the samples in Fig. 2a–c are shown in Figs. 3–5, where both carbon (top) and fluorine (bottom) EDS maps demonstrate the differences in both degree of penetration and distribution of PTFE between the various microstructures tested.

The PTFE is known to agglomerate near the surface [13], so it is not surprising that there is PTFE near the surfaces (top or bottom of the images) for most of the samples. Additionally, for Figs. 3–5, the through-plane direction is along the vertical axis of the images, and the images themselves are of cut cross-sections of GDL materials.

It is important to note that EDS is a surface technique, so only PTFE near the cross-sectional surface will be detected. Since the GDLs tested were highly porous, electron beams that did not impact near the surface dissipated within the irregular lattice structure of the materials. As a result, only PTFE near the surface could be detected. X-rays emitted from PTFE particles deep within the GDL would be lost due to the complex pore morphology.

EDS maps for the paper GDL are shown in Fig. 3a (carbon map) and Fig. 3b (fluorine map). PTFE was largely concentrated along the surface fibers (near the top and bottom surfaces), with less fluorine detected in the central region. This observation could explain the water retention in the GDL core region following purging, as seen by Buchi et al. [21]. This also agrees with work by Fishman and Bazylak regarding PTFE accumulation at the surface regions along the thickness direction of the GDL [13]. From a study on the effect of PTFE on the through-plane porosity profiles of uncompressed paper GDLs, the authors found that the porosity of treated paper GDLs decreased near the surfaces, compared to that of untreated paper GDLs. The core porosity, however, did not show a comparable trend. That study found that PTFE is non-uniformly distributed along the thickness of the paper GDL, with the particles primarily accumulating near the surfaces of the GDL.

Fig. 4 shows the EDS maps of (a) carbon and (b) fluorine for the Freudenberg felt GDL. As expected from the hydro-entanglement manufacturing process, the carbon fibers were oriented randomly throughout the through-plane direction (Fig. 4a). Similar to the paper GDL (Fig. 3), the PTFE coating in the felt GDL is concentrated near the top and bottom surfaces. However, there is a gradual decrease in the PTFE content from the surfaces to the core of the GDL.

EDS maps for the cloth GDL (Fig. 5) illustrate the differences in carbon fiber morphology and PTFE distribution for the paper GDL, compared to the paper and felt GDLs. In particular, the PTFE is not limited to the surface regions, and has accumulated along the weaves of the cloth. While the PTFE did not significantly penetrate into the woven yarns of the cloth, Fig. 5b shows that some PTFE

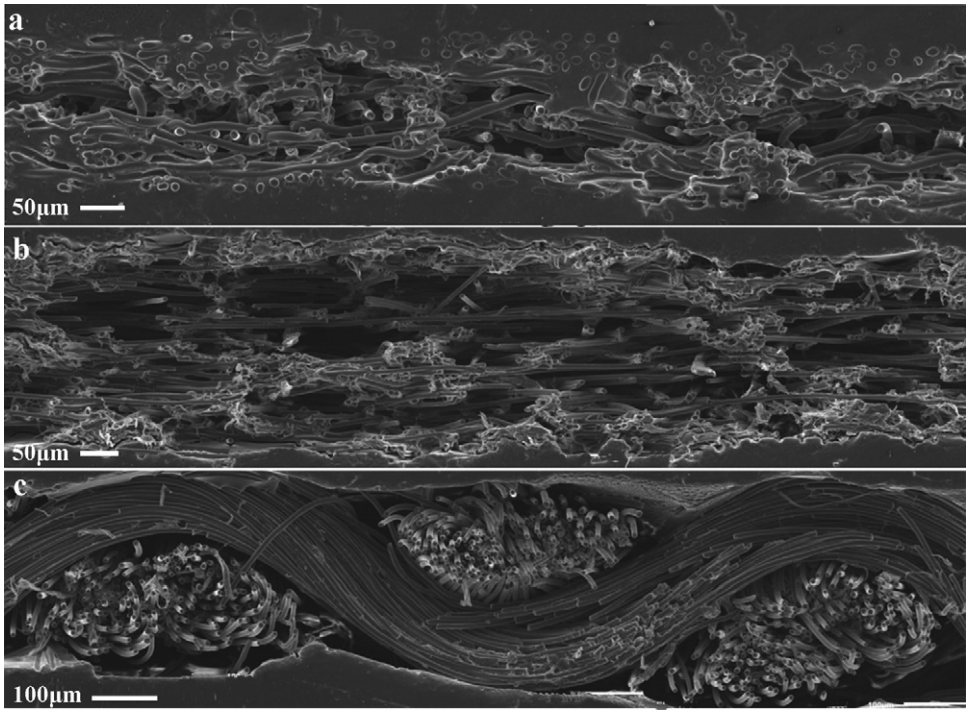

Fig. 2. SEIs from mold 1: (a) sample 1 (PTFE-treated felt, top); (b) sample 3 (PTFE-treated paper, middle); and (c) sample 5 (PTFE-treated cloth, bottom). Each image was measured as three adjacent measurements and combined to form the full image.

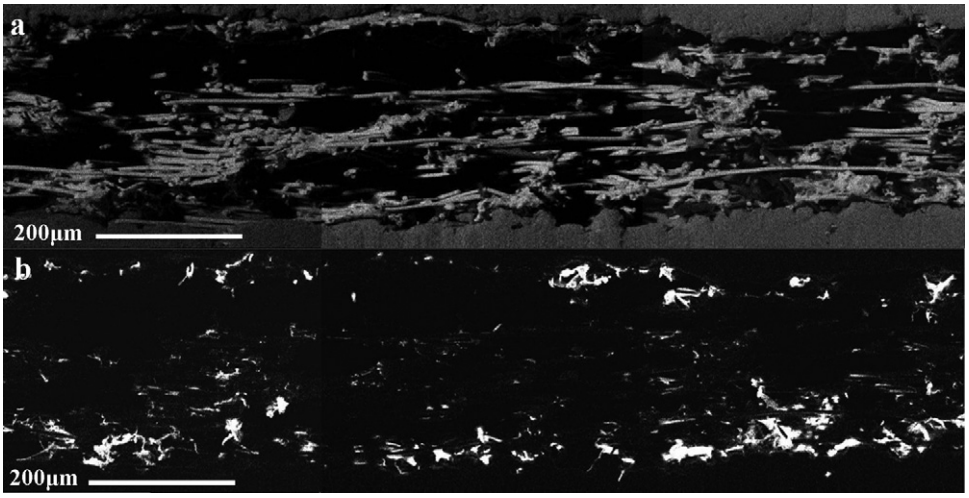

Fig. 3. The results of (a) carbon and (b) fluorine EDS maps on the paper GDL on mold 1. The carbon map appears much more detailed than the fluorine map due to the higher elemental presence of carbon, which composes most of the GDL. Each image was measured as three adjacent measurements and combined to form the full image. These images are cross-sections, so the through-plane direction is along the vertical axis of the image.

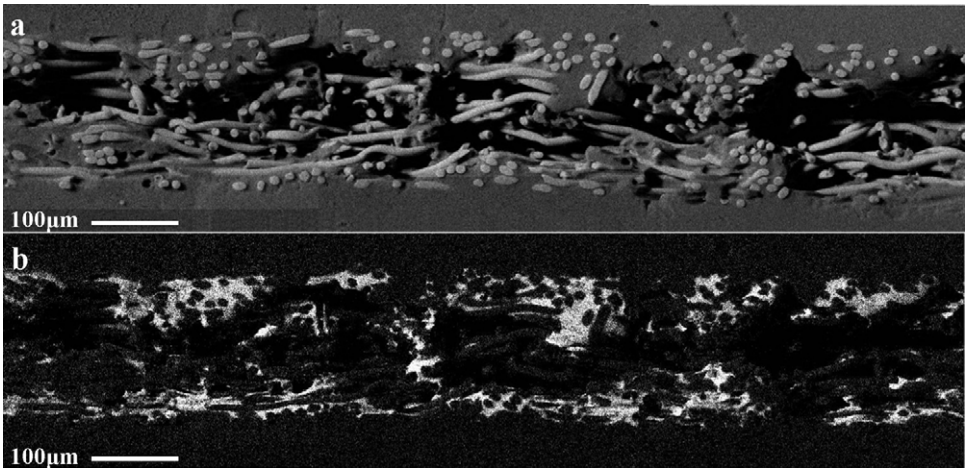

Fig. 4. The results of (a) carbon and (b) fluorine EDS maps on the felt GDL on mold 1. The carbon map appears much more detailed than the fluorine map due to the higher elemental presence of carbon, which composes most of the GDL. Each image was measured as three adjacent measurements and combined to form the full image. These images are cross-sections, so the through-plane direction is along the vertical axis of the image.

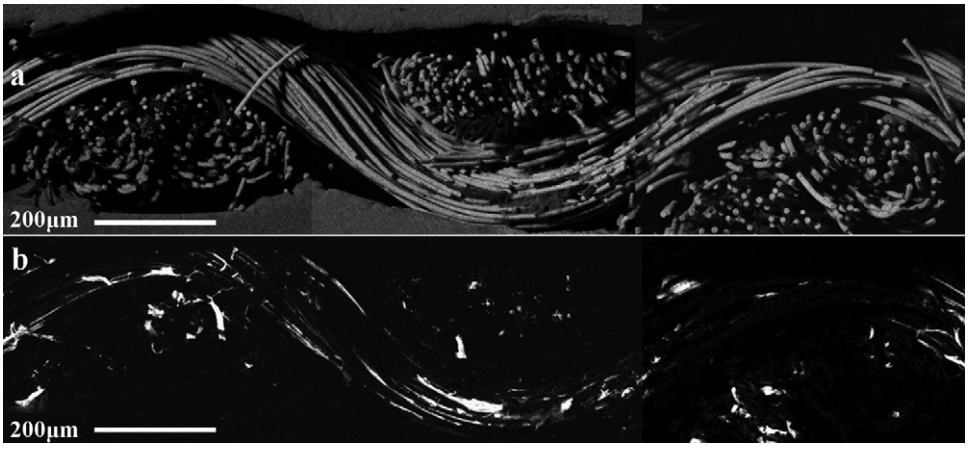

Fig. 5. The results of (a) carbon and (b) fluorine EDS maps on the cloth GDL on mold 1. The carbon map appears much more detailed than the fluorine map due to the higher elemental presence of carbon, which composes most of the GDL. Each image was measured as three adjacent measurements and combined to form the full image. These images are cross-sections, so the through-plane direction is along the vertical axis of the image.

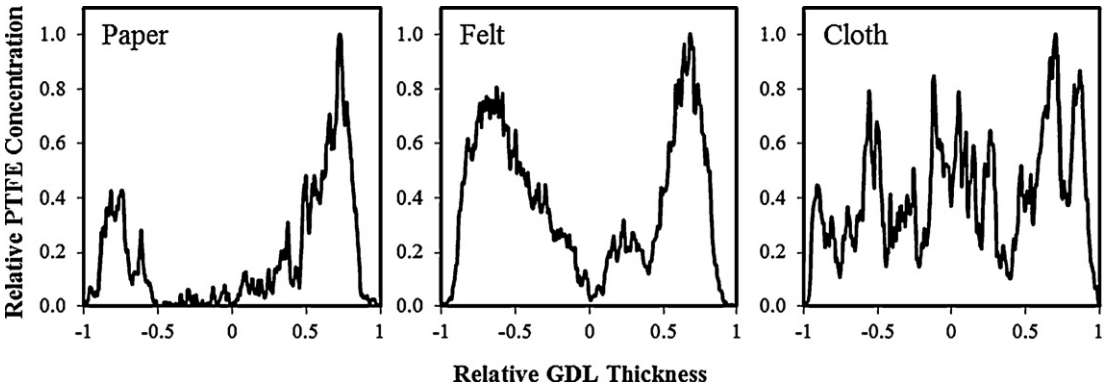

Fig. 6. Averaged through-plane PTFE distributions for the three treated GDL materials tested. The 0-position represents the center of the GDL.

did accumulate in the middle of the yarns, following the transverse fibers.

The SEM images discussed above provide a qualitative description of PTFE penetration into the various GDL microstructures. However, this does not provide a quantitative analysis of the actual PTFE content in the through-plane direction of the GDL. To highlight this information, fluorine distributions averaged along the in-plane direction of the images (along the horizontal axes in Figs. 3–5) are presented. The fluorine content and GDL thicknesses were normalized to facilitate comparison and standardize contrast effects introduced by the SEM software. This analysis was performed using a Matlab script, described in Section 2. The normalized distributions for the three microstructures (paper, felt, and cloth) are discussed below.

The distribution plots for the three GDL materials are shown in Fig. 6. It is important to note that, for this study, we are interested in relative PTFE distributions in the through-plane direction of the GDL. At present, quantification of the exact amounts or spatial locations of PTFE is beyond the scope of this study. The plot for paper demonstrates approximately symmetrical adsorption of PTFE within the sample, with peaking PTFE concentrations near the surface edges and lower accumulation in the core. A similar bimodal distribution is seen for the felt GDL. The PTFE penetration in the cloth, however, appears more uniform throughout the bulk of the GDL. This is likely due to the transverse weave pattern of the cloth, which is expanded in more detail below.

4. Discussion

We can attribute the symmetric, bimodal distribution in the felt and paper GDLs to (i) the drying time following PTFE application [5] and (ii) the surface morphology of the paper GDL, whereby the PTFE suspension easily penetrate into the surface pores [13,22]. Additionally, Fig. 6 shows higher concentrations of PTFE closer to the right hand surface side of the paper GDL. Further work is required to determine the specific cause of this imbalance, but it is likely related to the application methods used.

The PTFE distribution in felt is similarly bimodal; however, the PTFE was able to penetrate deeper into the felt than the paper. This suggests that the binder used in the papermaking process impedes the infiltration of PTFE distribution into the bulk of the paper GDL. In felt, there is no local surface porosity minima associated with binder [22] preventing the PTFE from penetrating deeper into the GDL core region. In contrast, for the surface regions of the paper GDL, local low-porosity binder regions cause PTFE to accumulate at the surface [13]. This is equally demonstrated in Fig. 6 for the paper and felt distributions. It can also be noted that the PTFE accumulates as large agglomerations in regions of densely packed fibers.

The uniform appearance of PTFE through the cloth sample shown in Fig. 6 is different than the bimodal distributions for the cloth and paper GDLs. The resulting distribution appears more uniform, with some fluctuations. However, this is an artifact of the sinusoidal pattern of the cloth weave. As can be seen from Fig. 5b, the fluorine of PTFE follows the carbon strands of the weave. Since the weave traverses the full through-plane thickness of the cloth, the averaged fluorine content appears to remain consistent throughout the GDL thickness. As well, the random nature of the distribution could be attributed to the fact that each scanned region of the cloth GDL contains significant amounts of in-plane and transversely oriented fibers, with some PTFE penetrating along the transverse yarns. PTFE does not appear to collect near the cloth GDL surface, as it does for paper and felt. Instead, PTFE is non-uniformly distributed along the in-plane and transverse strands of carbon fibers. Additionally, we cannot separate the through-plane region in cloth into surface and bulk regions because of the macro-porous structure created by the weave pattern of the fibers.

The technique reported here is capable of highlighting the locations of PTFE in all GDLs, including cloth. At present, however, the authors cannot comment on the effect that this would have on GDL performance, which is beyond the scope of this study. However, further *ex situ* experiments could be conducted to measure the diffusivity, permeability and porosity for cloth GDLs with variable PTFE loading and under PEMFC operating conditions. Improved PEMFC performance could be achieved by tailoring the PTFE distribution in the GDL to ensure that liquid water droplets do not interfere with diffusion through the GDL porous structure. Further investigation of the GDL is necessary for a complete characterization of the PTFE penetration. For instance, multiple through-plane slices of the GDL could be imaged by freeze-fracturing treated GDLs. Such a technique would minimize any damage to the PTFE or porous structure due to cutting processes, and would remove any possible surface agglomeration effects. Future work could also include an investigation of PTFE application methods, notably the drying time, temperature, and their impact on the imaged PTFE distribution.

5. Conclusion

In this work, we presented a novel method for measuring heterogeneous through-plane PTFE distributions within the bulk of the GDL using SEM-based EDS imaging. SEM EDS imaging and typical PTFE distributions for paper, felt, and cloth GDLs were presented and discussed. Paper and felt materials exhibited highly heterogeneous PTFE distributions in the through-plane direction, with high concentrations at the GDL surfaces and low concentrations in the core region. On the other hand, the PTFE distributions observed in cloth appeared to be significantly more consistent through the

thickness of the GDL. We have attributed the penetration of PTFE into the cloth GDL core to the weave pattern of the yarns, along which PTFE seemed to accumulate. SEI results were also provided to enable the comparison of PTFE distributions with the morphological features of the GDL. The results presented in this work can be used by modellers to inform their description of the anisotropic PTFE distributions throughout the GDL. This need for hydrophobicity distributions has been identified by Wang et al. in a recent review paper [14]. Additionally, the novel technique discussed here has the potential to allow manufacturers of GDL materials to parameterize their application of PTFE for optimal water management in the GDL. Ultimately, we hope that it will provide some insight into improving the overall design and performance of PEMFCs.

Acknowledgements

The Natural Sciences and Engineering Research Council of Canada (NSERC), Bullitt Foundation, Canada Foundation for Innovation (CFI), and University of Toronto are gratefully acknowledged for their financial support. The authors would also like to thank Mr. Zachary Fishman (University of Toronto) for helpful discussions and Mr. George Kretschmann for his imaging expertise.

References

[1] U.S. Department of Energy, Office of Fossil Energy, National Energy Technology Laboratory, Fuel Cell Handbook, 7th ed., EG&G Technical Services Inc., 2004, p. 427.
[2] S. Park, B.N. Popov, Fuel 88 (2009) 2068–2073.
[3] G. Lin, T. Van Nguyen, J. Electrochem. Soc. 152 (2005) A1942.
[4] L. Cindrella, A.M. Kannan, J.F. Lin, K. Saminathan, Y. Ho, C.W. Lin, J. Wertz, J. Power Sources 194 (2009) 146–160.
[5] M. Mathias, J. Roth, J. Fleming, W.L. Lehnert, in: W. Vielstich, A. Lamm, H.A. Gasteiger (Eds.), Handbook of Fuel Cells: Fundamentals, Technology, and Applications, Wiley, Chichester, England/Hoboken, NJ, 2003, pp. 1–21.
[6] J.Z. Fishman, H. Leung, A. Bazylak, Int. J. Hydrogen Energy 35 (2010) 9144–9150.
[7] S. Escribano, J. Blachot, J. Ethève, A. Morin, R. Mosdale, J. Power Sources 156 (2006) 8–13.
[8] J. Lobato, P. Cañizares, M. Rodrigo, C. Ruiz-López, J. Linares, J. Appl. Electrochem. 38 (2008) 793–802.
[9] R. Borup, J. Meyers, B. Pivovar, Y.S. Kim, R. Mukundan, N. Garland, D. Myers, M. Wilson, F. Garzon, D. Wood, P. Zelenay, K. More, K. Stroh, T. Zawodzinski, J. Boncella, J.E. McGrath, M. Inaba, K. Miyatake, M. Hori, K. Ota, Z. Ogumi, S. Miyata, A. Nishikata, Z. Siroma, Y. Uchimoto, K. Yasuda, K.I. Kimijima, N. Iwashita, Chem. Rev. 107 (2007) 3904–3951.
[10] M. Schulze, N. Wagner, T. Kaz, K.A. Friedrich, Electrochim. Acta 52 (2007) 2328–2336.
[11] C. Lim, C.Y. Wang, Electrochim. Acta 49 (2004) 4149–4156.
[12] Dupont Co., Fluoropolymer Comparison – Typical Properties, 2010, http://www2.dupont.com/Teflon_Industrial/en_US/tech_info/techinfo_compare.html.
[13] Z. Fishman, A. Bazylak, J. Electrochem. Soc. 158 (2011) B841–B845.
[14] Y. Wang, K.S. Chen, J. Mishler, S.C. Cho, X.C. Adroher, Appl. Energy 88 (2011) 981–1007.
[15] Dupont Co., Aqueous Dispersions, 2010, http://www2.dupont.com/Teflon_Industrial/en_US/products/product_by_name/teflon_ptfe/aqueous.html.
[16] Dupont Co., Teflon PTFE TE-3859, Aqueous Fluoropolymers made with Echelon™ Dispersion Technology, Dupont Co., Mississauga, Canada, 2006, http://www2.dupont.com/Teflon_Industrial/en_US/assets/downloads/k10918.pdf.
[17] Dupont Co., Teflon PTFE Coating, Extrusion and Molding, 2010, http://www2.dupont.com/Teflon_Industrial/en_US/products/product_by_name/teflon_ptfe/.
[18] S. Park, J. Lee, B.N. Popov, J. Power Sources 177 (2008) 457–463.
[19] A.J. Mendoza, M.A. Hickner, J. Morgan, K. Rutter, C. Legzdins, Fuel Cells (2011) 248–254.
[20] V. Radhakrishnan, P. Haridoss, Int. J. Hydrogen Energy 35 (2010) 11107–11118.
[21] F.N. Buchi, R. Fluckiger, D. Tehlar, F. Marone, M. Stampanoni, ECS Trans. 16 (2008) 587–592.
[22] Z. Fishman, J. Hinebaugh, A. Bazylak, J. Electrochem. Soc. 157 (2010) B1643–B1650.